Supplementary Information (SI) for Journal of Materials Chemistry A

This journal is © The Royal Society of Chemistry 20xx

Supporting information

Nano-graphdiyne derivative and natural amino acid molecule as bilateral charge transport layers dopants for efficient perovskite solar cells

Yadong Wang, [†*a] Guilin Hu, [†bc] Kaiyi Yang, [bc] Jiandong He, [bc] Cong Shao, [bc] Shengnan Fan, [bc] Jiaxin Ma, [bc] Yu Yuan, [bc] Jizheng Wang, [bc] and Yongjun Li *[bc]

[a] *School of Materials Science and Engineering, North China University of Water Resources and Electric Power, Zhengzhou 450045, China*
[b] *Beijing National Laboratory for Molecular Sciences, CAS Key Laboratory of Organic Solids, Institute of Chemistry, Chinese Academy of Sciences (ICCAS), Beijing 100190, China*
[c] *University of Chinese Academy of Sciences, Beijing 100049, China*

† These authors contributed equally to this work.

*E-mail: wangyadong@ncwu.edu.cn; liyj@iccas.ac.cn

Experimental Section

1. Materials

The SnO_2 colloid solution (15%), isopropanol (IPA), N, N-dimethylformamide (DMF) and dimethyl sulfoxide (DMSO) were purchased from Alfa Aesar. Serine was was obtained from Aladdin. Cesium iodide (CsI), Lead iodide (PbI_2), Formamidinium iodide (FAI), methylammonium bromide (MABr), methylammonium chloride (MACl), bis(trifluoromethane)sulfonimide lithium salt (Li-TFSI), 4-tertbutylpyridine (tBP), 2,2′,7,7′-tetrakis (N, N′-di-p-methoxy-phenylamine)-9,9′-spirobifluorene (Spiro-OMeTAD) and 4-methoxy-phenethylammonium iodide (CH_3O-PEAI) were all purchased from Xi'an Yuri Solar Co., Ltd. Acetonitrile was purchased from Acros Organics. Chlorobenzene (CB) was brought from Sigma Aldrich.

2. Synthesis of o-TB-GDY

The o-TB-GYD was synthesized according to our previously reported procedure [1]. It was prepared via the sixfold intramolecular Eglinton coupling reaction in the hexabutadiyne precursors that were obtained by the sixfold Cadiot-Chodkiewicz crosscoupling of hexaethynylbenzene.

Synthesis of o-TB-GDY precursor 4c. Compound 3c (3.08 g, 4.5 mmol) was dissolved in toluene (30 mL) and N, N-diisopropylethylamine (3 mL). The mixture was stirred under argon atmosphere for 15 minutes. Subsequently, $Pd(dba)_2 \cdot CHCl_3$ (15 mg, 0.014 mmol) and CuI (5 mg, 0.026 mmol) were added. Then, a solution of HEB (167 mg, 0.75 mmol) in DMF (5 mL) was added dropwise. The reaction mixture was stirred at room temperature for 40 h. After completion, the mixture was diluted with dichloromethane and washed sequentially with aqueous ammonium chloride solution and brine. The combined organic layers were dried over anhydrous sodium sulfate, and the solvent was removed under reduced pressure. Purification by silica gel column chromatography (eluent: petroleum ether/ethyl acetate, gradient from 3:1 to 1:1) afforded the compound 4c (1.13 g, 39% yield). ^1H NMR (400 MHz, $CDCl_3$) δ 7.66 (s, 6H), 7.59 (d, J = 8.2 Hz, 18H), 7.47 (d, J = 8.3 Hz, 12H), 7.38 (d, J = 8.0 Hz, 6H), 7.30 (d, J = 8.3 Hz, 12H), 7.12 (s, 12H), 7.07 (d, J = 8.2 Hz, 12H), 3.17 – 2.46 (m, 12H), 1.60 (s, 72H), 1.37 (s, 54H), 1.30 (s, 54H). ^{13}C NMR (101 MHz, $CDCl_3$) δ 150.78, 150.20, 142.51, 141.15, 140.91, 137.54, 137.27, 136.40, 132.66, 130.58, 129.49, 129.31, 129.20, 126.77, 126.66, 125.95, 125.84, 125.17, 124.60, 99.24, 85.37, 84.94, 80.93, 79.91, 79.09, 65.61, 60.39, 34.60, 34.55, 31.37.

Under stirring and argon protection, o-TB-GDY precursor 4c (77 mg, 0.02 mmol) and KOH (25 mg, 0.45 mmol) were added to dry toluene (50 mL). The mixture was heated at 120 °C for 15 min and then cooled to room temperature. The reaction mixture was filtered through a short silica gel pad, and the filtrate was concentrated to approximately 20 mL for immediate use in the next step. The deprotected precursor solution was added dropwise via a syringe pump over 16–20 h to a suspension of CuCl (117.6 mg, 1.2 mmol) and $Cu(OAc)_2 \cdot H_2O$ (238.8 mg, 1.2 mmol) in pyridine (250 mL) maintained at 60°C. After the addition was complete, the mixture was concentrated under reduced pressure and diluted with dichloromethane. The organic layer was washed sequentially with 10% HCl (aq) and repeatedly with deionized water. It was then dried over $MgSO_4$, filtered, concentrated, and purified by column chromatography (eluent: petroleum ether/CH_2Cl_2 = 1:1) to afford o-TB-GDY (42 mg, 67% yield). ^1H NMR (700 MHz, CS_2/CD_2Cl_2 (25/1 v/v), 298 K) δ 7.61 (s, 6H), 7.59 (d, 6H), 7.52 (d, J = 7.0 Hz, 12H), 7.43 (d, J = 7.5 Hz, 12H), 7.32 – 7.29 (m, 6H), 7.26 (d, J = 8.1 Hz, 12H), 7.14 (s, 12H), 7.07 (d, 12H), 1.45 (s, 54H), 1.31 (s, 54H). ^{13}C NMR (176 MHz, CS_2/CD_2Cl_2 (25/1 v/v), 298 K) δ 150.78, 150.41, 141.75, 141.54, 137.84, 137.11, 134.26, 131.70, 130.23, 129.98, 127.65, 127.55, 127.24, 126.54, 126.46, 126.11, 86.73, 84.28, 82.89, 81.12, 80.75, 79.74, 34.93, 34.83, 32.21, 32.04.

3. SnO_2-Serine solution preparation

The SnO_2 colloid precursor was diluted with deionized water, and the volume ratio is 120:650. Serine dispersion was prepared by dispersing serine (10 mg) in deionized water (1 mL) and then sonicating at 25°C for 30 min. Serine dispersion was used to prepare the SnO_2-Serine solution with appropriate doping concentrations (0, 0.5, 2.5, and 5.0 mg mL^{-1}).

4. Spiro-OMeTAD-GDY solution preparation

The Spiro-OMeTAD precursor solution was prepared by dissolving 72.3 mg Spiro-OMeTAD, 35 µL Lithium bis(trifluoromethylsulfonyl)imide salt solution (260 mg Li-TFSI dissolved in 1 mL acetonitrile), 28.8 µL 4-tertbutylpyridine, and 1 mL CB. o-TB-GDY dispersion was prepared by dispersing o-TB-GDY (1 mg) in CB (1 mL) and then sonicating at 25°C for 24 h. o-TB-GDY dispersion was subsequently used to prepare the Spiro-OMeTAD-GDY solution with different doping concentrations (0, 0.01, 0.05, and 0.10 mg mL^{-1}).

5. Device fabrication

The ITO substrates were ultrasonically washed with deionized water, acetone and isopropanol for 15 min in sequence. After that, the substrates were treated by oxygen plasma for 10 min. The SnO_2 colloid precursor was diluted with deionized water, and the volume ratio is 120:650. The SnO_2 or SnO_2-Serine thin layer was prepared by spin-coating the SnO_2-Serine solution on the ITO substrates at 3500 rpm for 30 s, and then annealed at 150°C for 30 min. The perovskite films were prepared by a two-step spin-coating program. Firstly, 704 mg PbI_2 and 16.9 mg CsI were dissolved in a mixed solvent of DMF (1 mL) and DMSO (160 µL). The PbI_2 precursor solution was heated at 60°C for 12 h and then filtered using a 0.22 µm pore PTFE filter. The 60 µL PbI_2 precursor solution was spin-coated onto the SnO_2 with or without serine doping substrate at 1600 rpm for 20 s and 4000 rpm for 30 s successively in the N_2-filled glove box. The obtained PbI_2 film was annealed at 70°C for 2 min. Secondly, for the mixed organic amine salt solution, 110 mg FAI, 11.5 mg MACl, and 11 mg MABr were dissolved in 1500 µL isopropanol and then ultrasonically treated for 30 min. It was filtered with a 0.22 µm PTFE filter and spin-coated on the PbI_2 layer at 2000 rpm for 25 s. Then the perovskite film was transferred from the N_2-filled glove box to ambient air (30~40% relative humidity) and annealed at 140°C for 20 min. After annealing, the film was transferred back to the N_2-filled glove box. 100 µL CH_3O-PEAI isopropanol solution with the concentration of 3 mg mL^{-1} was spin-coated onto the perovskite film at 4000 rpm for 30 s, and then annealed at 100°C for 5 min. Then the control Spiro-OMeTAD or Spiro-OMeTAD-GDY film was prepared by spin-coating the corresponding precursor solution on the top of perovskite film at 4000 rpm for 30 s. After that, the sample was kept in a desiccator for 1 day. Finally, the 70 nm Au electrode was deposited on the control Spiro-OMeTAD or Spiro-OMeTAD-GDY layer by thermal evaporation.

6. Characterizations

^1H and ^{13}C NMR spectra were acquired on Bruker Fourier 300, AVANCE 400, or Bruker NEO 700 NMR spectrometers maintained at 25°C. Matrix-assisted laser desorption/ionization Fourier transform ion cyclotron resonance (MALDI-FT-ICR-MS) mass spectrometry were performed on a Bruker Solarix 9.4T FT-ICR-MS mass spectrometer. Ultraviolet/visible absorption (UV-vis) spectra were acquired by a SHIMADZU UV-2600 spectrophotometer. X-ray diffraction (XRD) patterns were recorded by a Rigaku-2500 X-ray diffractometer. X-ray photoelectron spectroscopy (XPS) spectra were characterized by d using a Thermo Scientific ESCALab 250Xi. Ultraviolet photoelectron spectroscopy (UPS) results were characterized by a UPS machine (AXIS ULTRA DLD, Kratos). The UV light source used is He I, and the energy of He I is 21.22 eV. Scanning electron microscopy (SEM) images were acquired by a Hitachi S-4800 microscope. Atomic force microscopy (AFM) images of perovskite films were characterized by a NanoScope IIIa in tapping mode. Steady-state PL spectra and time-resolved PL spectra were obtained by a FLS980 fluorescence spectrometer system (Edinburgh Instruments Ltd.). Grazing incidence wide-angle X-ray scattering (GIWAXS) patterns were acquired by a Xeuss 2.0 SAXS/WAXS system (Xenocs SA, France). External quantum efficiency (*EQE*) curves were recorded by a Newport 300 W Xenon Light Source (Newport IQE 200, USA). *J-V* curves of the PSCs were measured using a source meter (Keithley 2420, USA) under AM 1.5G sunlight at an irradiance of 100 mW cm^{-2} provided by a solar simulator (Newport, Oriel Sol3A Class AAA, 94043A). Light intensities were calibrated using a monocrystalline silicon reference cell (Newport, Oriel 91150). The device area of PSCs is 0.04 cm^{-2}.

7. Calculation Method

The electrostatic potential (ESP) of serine molecule and o-TB-GDY were calculated according to the previous literatures [2, 3]. All density functional theory (DFT) calculations were performed in the CP2K code and using a hybrid Gaussian and plane-wave basis sets [4-6]. Core electrons were treated with norm-conserving Goedecker-Teter-Hutter pseudopotentials, while valence electron wavefunction were expressed in a double-zeta basis set with polarization functions and an auxiliary plane-wave basis set (energy cutoff = 500 eV). The Perdew-Burke-Enzerhof (PBE) generalized gradient approximation exchange-correlation functional was used. The models were builded based on the (100) crystal plane of $CsFAMAPbI_3$ with a 4*4*1 supercell. Configurations were optimized using the Broyden-Fletcher-Goldfarb-Shanno (BGFS) algorithm with SCF convergence criteria of 1.0×10^{-5} au. Grimme's DFT-D3 van der Waals correction was also employed.

The binding energy (*BE*) between SnO_2, perovskite, and dopants were calculated using the following equation:

$$BE = E_{adsorbate + substrate} - E_{adsorbate} - E_{substrate} == \quad (1)$$

Where $E_{adsorbate+substrate}$, $E_{adsorbate}$ or $E_{substrate}$ represents the total energy of the substrate with the adsorption of adsorbate, adsorbate and substrate, respectively.

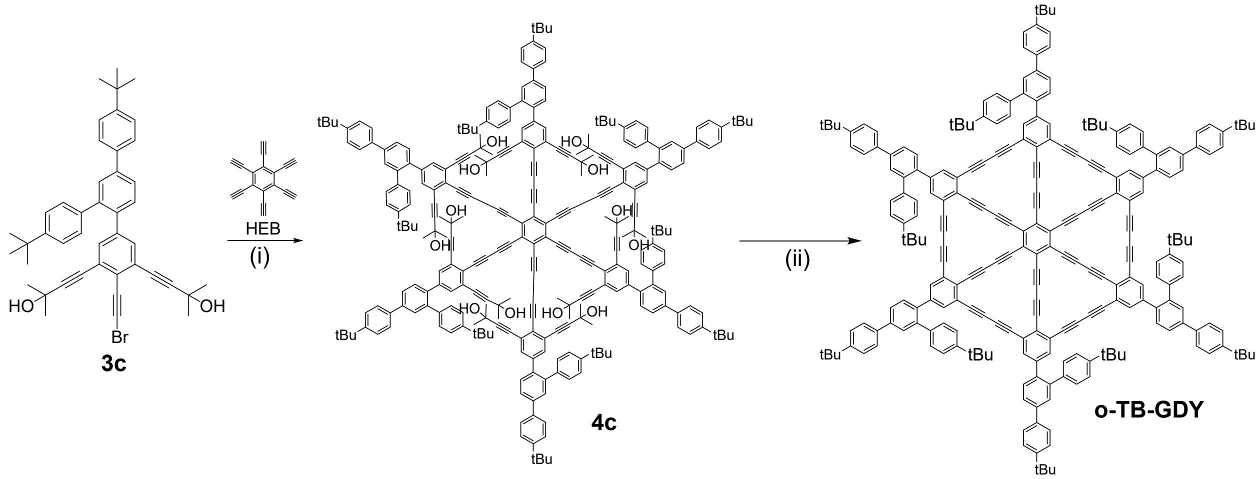

Fig. S1 Synthetic route of o-TB-GDY. This synthetic route was consistent with our previous work (*J. Am. Chem. Soc.* 2023, **145**, 5400-5409). Reaction conditions: (i) hexaethynylbenzene/DMF, Pd(dba)$_2$•$CHCl_3$, CuI, N,N-diisopropylethylamine, toluene, RT, 40 h; (ii) (a) KOH, toluene, 120℃, 15 min; (b) CuCl (60 equiv) and Cu(OAc)$_2$•H_2O (60 equiv), pyridine, 60℃. Compound 3c was synthesized according to the procedure reported in *J. Am. Chem. Soc.* 2023, **145**, 5400-5409; compound hexaethynylbenzene (HEB) was prepared following the method described in *Chem. Commun*. 2010, **46**, 3256-3258.

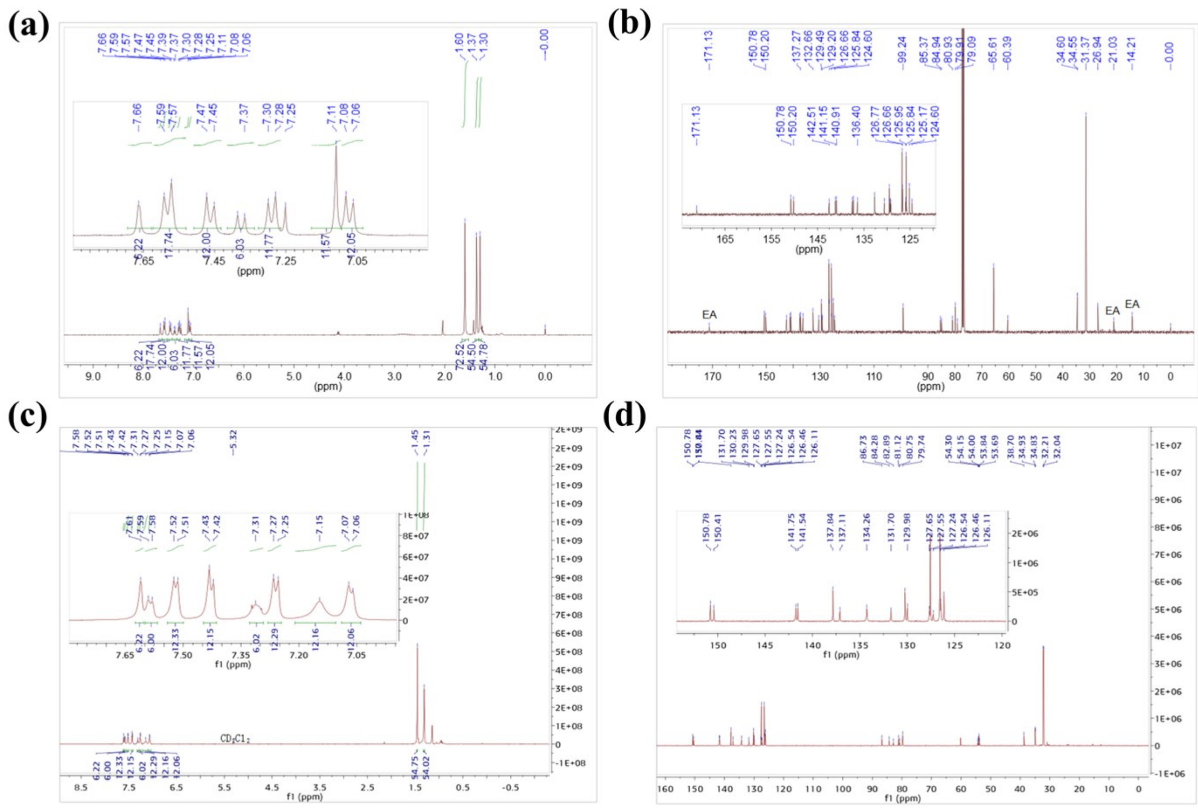

Fig. S2 ^{1}H and ^{13}C NMR spectra of precursor 4c and o-TB-GDY. The data are consistent with those reported in the literature (*J. Am. Chem. Soc.* 2023, **145**, 5400-5409). (a) ^{1}H NMR (400 MHz, $CDCl_3$) spectrum of compound 4c at 298 K. (b) ^{13}C NMR (101 MHz, $CDCl_3$) spectrum of compound 4c at 298 K. (c) ^{1}H NMR (700 MHz, CS_2/CD_2Cl_2 (25/1 v/v), 298 K) spectrum of compound o-TB-GDY at 298 K. ^{13}C NMR (176 MHz, CS_2/CD_2Cl_2 (25/1 v/v), 298 K) spectrum of compound o-TB-GDY at 298 K.

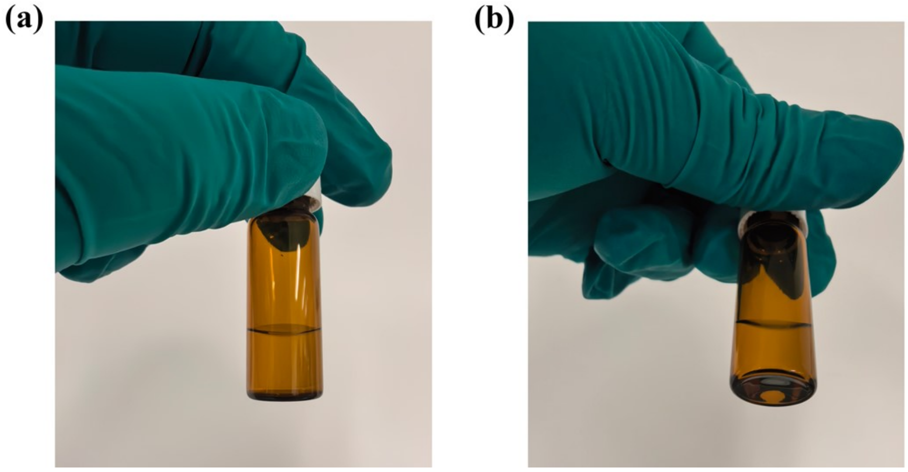

Fig. S3 Optical images of serine dispersed in SnO_2 aqueous solution (5.0 mg mL^{-1}) observed from (a) upright and (b) oblique perspectives.

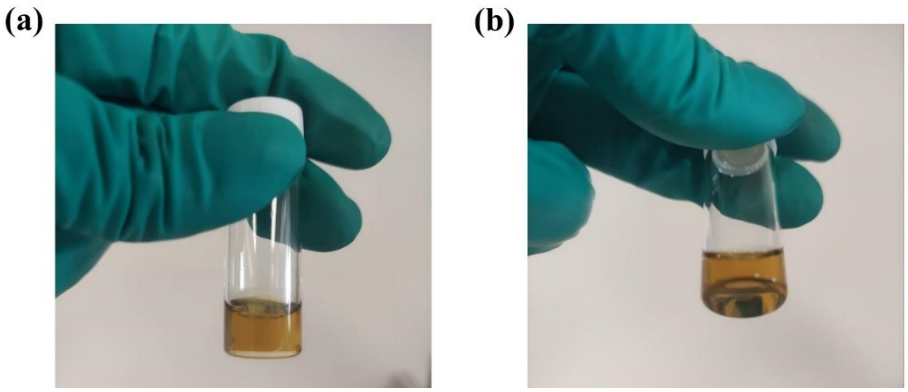

Fig. S4 Optical images of o-TB-GDY dispersed in chlorobenzene (0.10 mg mL^{-1}) observed from (a) upright and (b) oblique perspectives.

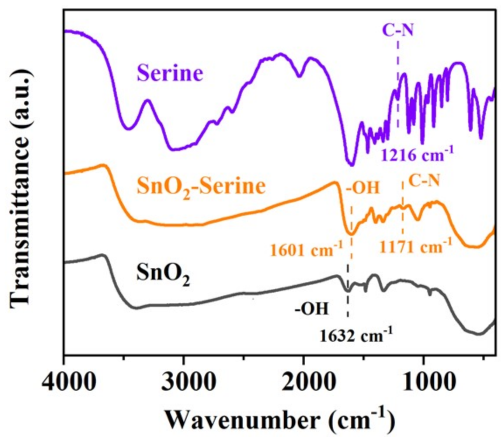

Fig. S5 FTIR spectra of the (a) serine, SnO_2, and SnO_2-serine samples.

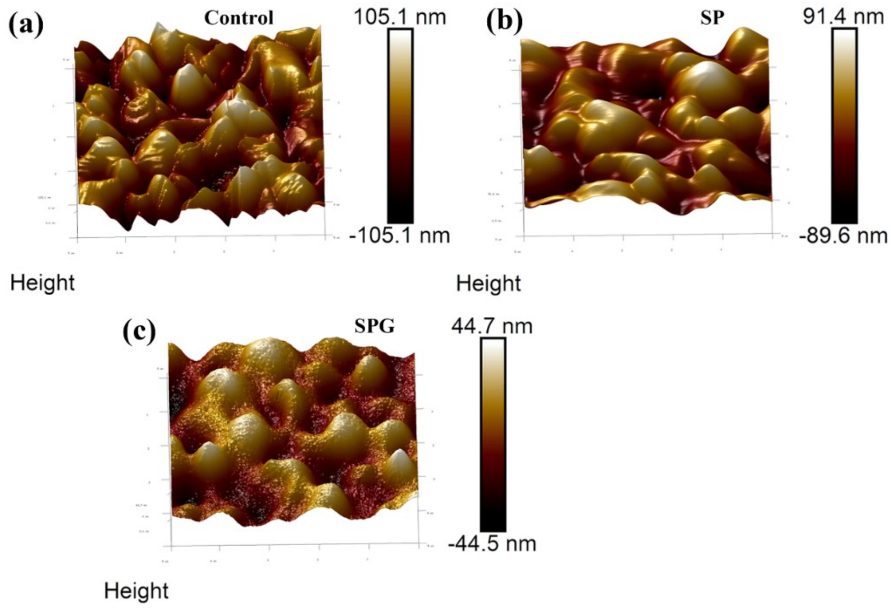

Fig. S6 3D AFM images of the (a) control, (b) SP, and (c) SPG films.

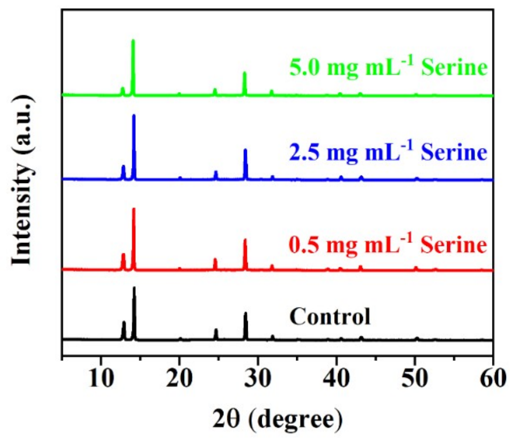

Fig. S7 X-ray diffraction patterns of perovskite films treated with various concentrations of serine.

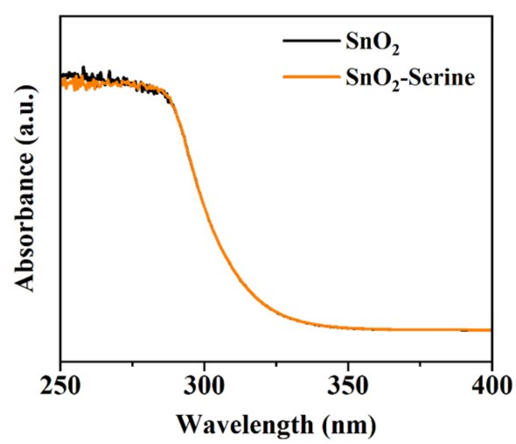

Fig. S8 UV-visible absorption spectra of the SnO_2 and SnO_2-Serine ETLs.

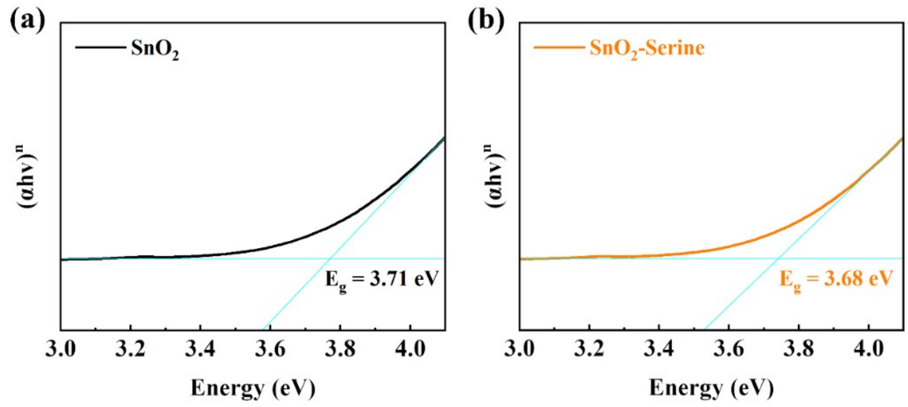

Fig. S9 Tauc plots for (a) SnO_2 and (b) SnO_2-Serine ETLs.

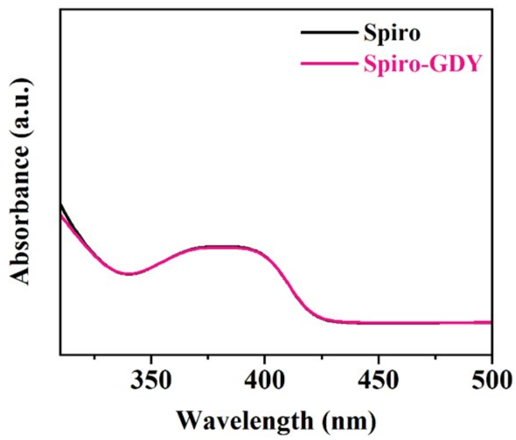

Fig. S10 UV-visible absorption spectra of the Spiro-OMeTAD and Spiro-OMeTAD-GDY HTLs.

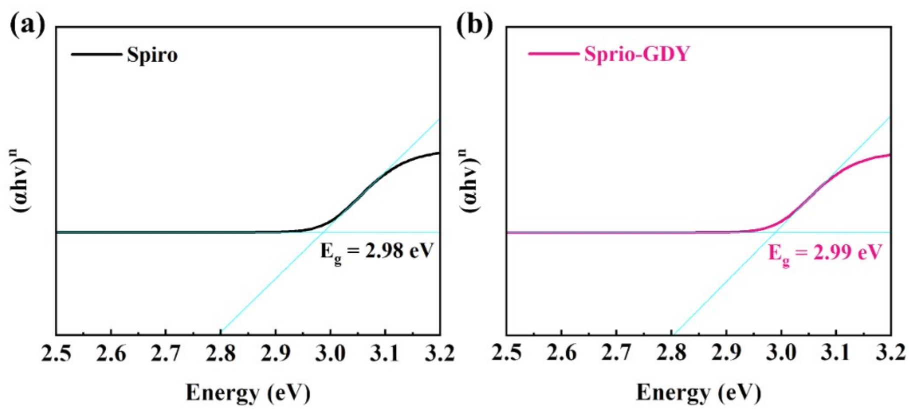

Fig. S11 Tauc plots for (a) Spiro-OMeTAD and (b) Spiro-OMeTAD-GDY HTLs.

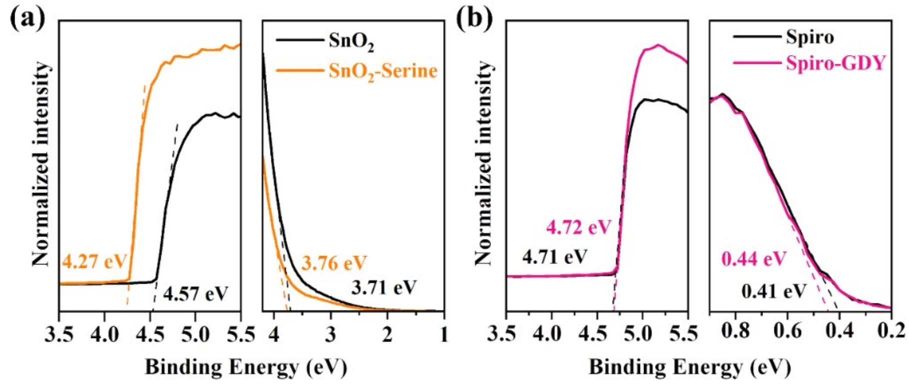

Fig. S12 Work function and HOMO results of the (a) SnO_2 and SnO_2-Serine ETL films and (b) Spiro-OMeTAD and Spiro-OMeTAD-GDY HTL films.

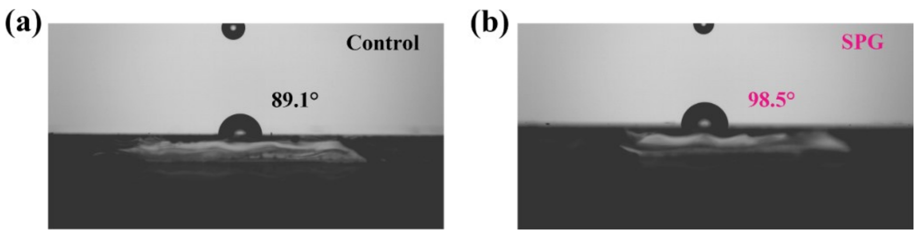

Fig. S13 The contact angle measurements of the (a) control and (b) SPG films.

Table S1 The summarized band structure parameters for control perovskite and SPG-based films.

Sample	WF (eV)	E_c (eV)	E_v (eV)	HOMO (eV)
SnO_2	4.57	4.57	8.28	3.71
SnO_2-Serine	4.27	4.35	8.03	3.76
Sprio-OMeTAD	4.71	2.14	5.12	0.41
Sprio-OMeTAD-GDY	4.72	2.17	5.16	0.44

Table S2 Summaries of fitting parameters for TRPL spectra based on different ETLs.

Sample	A_1	τ_1 (ns)	A_2	τ_2 (ns)	τ_{ave} (ns)
SnO_2/perovskite	68.89	130.62	521.40	601.24	588.11
SnO_2-Serine/perovskite	209.36	106.01	347.05	385.84	346.05

Table S3 Summaries of fitting parameters for TRPL spectra based on different HTLs.

Sample	A_1	τ_1 (ns)	A_2	τ_2 (ns)	τ_{ave} (ns)
Sprio-OMeTAD	235.63	49.34	385.89	326.64	303.21
Sprio-OMeTAD-GDY	862.84	22.43	251.64	270.96	216.01

Table S4 Performances of the PSCs based on the films doping with various concentrations of serine.

Sample	V_{oc} (V)	J_{sc} (mA cm^{-2})	FF (%)	PCE (%)
Control	1.165±0.016	23.96±0.375	78.54±1.16	21.93±0.46
0.5 mg mL^{-1}	1.174±0.006	24.25±0.779	79.87±1.63	22.74±0.42
2.5 mg mL^{-1}	1.183±0.013	24.18±0.528	80.47±0.71	23.01±0.38
5.0 mg mL^{-1}	1.161±0.011	24.62±0.504	79.23±1.41	22.65±0.29

Table S5 Performances of the PSCs based on the films doping with various concentrations of o-TB-GDY.

Sample	V_{oc} (V)	J_{sc} (mA cm^{-2})	FF (%)	PCE (%)
Control	1.165±0.016	23.96±0.375	78.54±1.16	21.93±0.46
0.01 mg mL^{-1}	1.218±0.004	23.93±0.390	79.34±1.13	23.14±0.36
0.05 mg mL^{-1}	1.219±0.005	24.39±0.413	79.58±0.64	23.67±0.29
0.10 mg mL^{-1}	1.215±0.009	24.43±0.453	79.34±0.95	23.48±0.38

Table S6 Photovoltaic parameters of champion control and SPG-based PSCs.

Sample	Scan Direction	V_{oc} (V)	J_{sc} (mA cm^{-2})	FF (%)	PCE (%)	Hysteresis Index (%)
SPG	Reverse	1.227	24.72	80.68	24.46	2.29
	Forward	1.220	24.74	79.16	23.90	
Control	Reverse	1.161	24.63	78.67	22.50	5.87
	Forward	1.147	24.45	75.47	21.18	

Table S7 EIS parameters of the control and SPG-based devices.

Sample	R_s (Ω)	R_{tr} (Ω)	C_{tr} (F)	R_{rec} (Ω)	C_{rec} (F)
Control	40.0	49.9	4.26×10^{-9}	1.13	3.47×10^{-9}
SPG	65.4	40.2	5.21×10^{-9}	2.45	3.15×10^{-9}

References

1 G. L. Hu, J. Y. He, J. Chen and Y. J. Li, *J. Am. Chem. Soc.*, 2023, **145**, 5400-5409.

2 C. Shao, J. Y. He, J. X. Ma, Y. R. Wang, G. S. Niu, P. F. Zhang, K. Y. Yang, Y. Zhao, F. Y. Wang, Y. J. Li and J. Z. Wang, *Nano-Micro Lett.*, 2025, **17**, 121.

3 G. Xing, C. B. Li, W. Y. Gao, J. X. Yang, X. J. Zhao, J. P. Wang, X. Q. Ran, L. F. Chao, H. Huang, Y. P. Zhou, Y. H. Chen, Z. B. Wu, C. X. Ran and W. Huang, *Adv. Mater.*, 2024, **36**, 2404185.

4 S. Yang, J. D. He, Z. H. Chen, H. Luo, J. B. Wei, X. Y. Wei, H. Li, J. D. Chen, W. F. Zhang, J. Z. Wang, S. Wang and G. Yu, *Adv. Mater.*, 2024, **36**, 2408686.

5 X. Song, R. Y. Wang, X. Wang, H. Y. Han, Z. Y. Qiao, X. W. Sun and W. H. Ji, *J. Hazard. Mater.*, 2022, **423**, 127226.

6 Y. L. Zhao, Y. Y. Wang, W. J. Xue, R. Y. Cheng, X. Zheng, G. C. Zhu, D. Y. Hu, H. L. Huang, C. G. Hu and D. Liu, *Adv. Mater.*, 2024, **36**, 2403097.